

## Use of a Pharmacophore Model for the Design of EGFR Tyrosine Kinase Inhibitors: Isoflavones and 3-Phenyl-4(1*H*)-quinolones

Peter Traxler,<sup>\*,†</sup> Jennifer Green,<sup>‡</sup> Helmut Mett,<sup>†</sup> Urs Séquin,<sup>‡</sup> and Pascal Furet<sup>\*,†</sup>

NOVARTIS Pharmaceuticals, Therapeutic Area Oncology, NOVARTIS Limited, CH-4002 Basel, Switzerland, and Institute of Organic Chemistry, University of Basel, CH-4056 Basel, Switzerland

Received September 29, 1998

Using a pharmacophore model for ATP-competitive inhibitors interacting with the active site of the EGFR protein tyrosine kinase together with published X-ray crystal data of quercetin (**2**) in complex with the Hck tyrosine kinase and of deschloroflavopiridol (**3b**) in complex with CDK2, a putative binding mode of the isoflavone genistein (**1**) was proposed. Then, based on literature data suggesting that a salicylic acid function, which is represented by the 5-hydroxy-4-keto motif in **1**, could serve as a pharmacophore replacement of a pyrimidine ring, superposition of **1** onto the potent EGFR tyrosine kinase inhibitor 4-(3'-chlorophenylamino)-6,7-dimethoxyquinazoline (**4**) led to 3'-chloro-5,7-dihydroxyisoflavone (**6**) as a target structure which in fact was 10 times more potent than **1**. The putative binding mode of **6** suggests a sulfur–aromatic interaction of the *m*-chlorophenyl moiety with Cys 773 in the “sugar pocket” of the EGFR kinase model. Replacement of the oxygen in the chromenone ring of **6** by a nitrogen atom further improved the inhibitory activity against the EGFR kinase. With IC<sub>50</sub> values of 38 and 8 nM, respectively, the quinolones **11** and **12** were the most potent compounds of the series. *N*-Alkylation of **11** did not further improve enzyme inhibitory activity but led to derivatives with cellular activity in the lower micromolar range.

### Introduction

Protein tyrosine kinases (PTK) play a fundamental role in signal transduction pathways. Deregulated PTK activity has been observed in many proliferative diseases (e.g., cancer, psoriasis, restenosis, etc.).<sup>1</sup> A number of tumor types have dysfunctional growth factor receptor PTKs which results in inappropriate mitogenic signaling. Tyrosine kinases are therefore attractive targets for the design of new therapeutic agents against cancer.<sup>2,3</sup> The EGFR PTK was one of the first tyrosine kinases described in the literature and was therefore chosen as a target by many companies to start research programs in the signal transduction area.

The family of the epidermal growth factor receptor (EGFR) PTK belongs to the large class of the transmembrane growth factor receptor PTKs. This EGFR family contains four members: the EGFR kinase (*c-erbB1* gene product), the p185<sup>erbB2</sup> (*c-erbB2* gene product), and the *c-erbB3* and *c-erbB4* gene products. The EGFR and its ligands (EGF, TGF- $\alpha$ ) have been implicated in numerous tumors of epithelial origin (e.g., squamous cell carcinoma; breast, ovarian, and NSC lung cancer)<sup>1,4</sup> and proliferative disorders of the epidermis such as psoriasis.<sup>5</sup> The EGFR and *c-erbB2* PTKs have been identified as interesting targets for medicinal chemistry programs. Inhibitors of the EGFR PTK are therefore expected to have great therapeutic potential in the treatment of malignant and nonmalignant epithelial diseases.

Within the great number of different structural classes of tyrosine kinase inhibitors which have been

reported and reviewed in the past few years,<sup>3,6–10</sup> compounds competing with ATP for binding at the catalytic domain are considered to be of great interest. Numerous examples of structurally diverse classes have proved to be highly potent and selective ATP-competitive tyrosine kinase inhibitors. Interest has focused on a special group of compounds containing a (phenylamino)pyrimidine moiety in their structures such as (phenylamino)quinazolines,<sup>11–14</sup> 7-amino-4-(phenylamino)pyrido[4,3-*d*]pyrimidines,<sup>15,16</sup> 4-(phenylamino)pyrimido[5,4-*d*]pyrimidines,<sup>17</sup> 4-(phenylamino)pyrrolo[2,3-*d*]pyrimidines,<sup>18</sup> and 4-(phenylamino)pyrazolo[3,4-*d*]pyrimidines.<sup>19</sup> Meanwhile, the first quinazoline derivatives have entered clinical trials as anticancer agents (e.g., Zeneca ZD 1839<sup>20</sup> and Pfizer/Oncogene CP 358774<sup>21</sup>), and several compounds of the other classes are in late stage of preclinical development.

Although more than 30 crystal structures of protein kinases complexed with ATP or an ATP-competitive inhibitor have been published in the past few years, no crystal structure of the EGFR has yet appeared. In 1995, Furet et al. (Novartis) published the first data of their pharmacophore model for inhibitors competing with the ATP-binding site of the EGFR PTK.<sup>22</sup> This model has then successfully been used for the design and synthesis of 4-(phenylamino)pyrrolopyrimidines<sup>18</sup> and 4-(phenylamino)pyrazolo[3,4-*d*]pyrimidines.<sup>19</sup> In parallel, Parke-Davis scientists proposed a model for the binding of 4-(phenylamino)quinazolines, 4-(phenylamino)pyrido[4,3-*d*]pyrimidines,<sup>23</sup> or pyrido[2,3-*d*]pyrimidines<sup>24</sup> at the ATP-binding site of the EGFR tyrosine kinase.

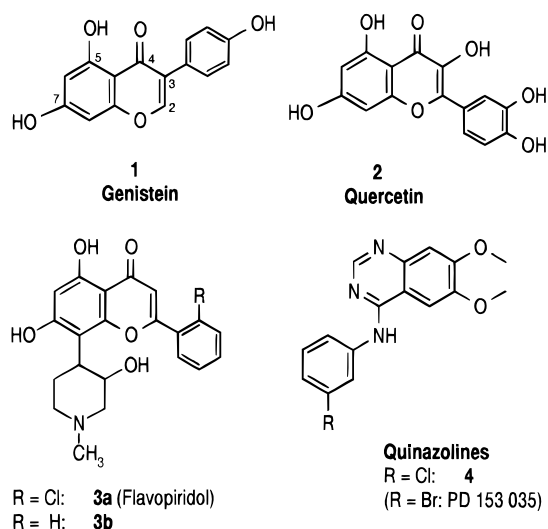
In the present paper, we describe another successful application of our pharmacophore model leading to a hypothetical binding mode for genistein and to the design and synthesis of 3'-chloro-5,7-dihydroxyisofla-

\* To whom correspondence should be addressed. Dr. Peter Traxler: phone, +41 61/696 52 86; fax, +41 61/696 34 29. Dr. Pascal Furet (molecular modeling): phone, +41 61/696 7990; fax, +41 61/696 2761.

<sup>†</sup> NOVARTIS Ltd.

<sup>‡</sup> University of Basel.

## Chart 1



as well as 3-aryl-4(1*H*)-quinolones as potent and selective EGFR tyrosine kinase inhibitors.

## Design of Inhibitors

In previous work, we proposed a pharmacophore model for the inhibitors of the EGFR PTK that are ATP-competitive.<sup>10,18,19,22</sup> Using this model, we showed that potent inhibitors could be obtained with molecules presenting the following structural features:

—Hydrogen-bonding groups mimicking the N1 and N6 nitrogens of the adenine ring of ATP which are engaged in hydrogen bonds with the peptide backbone of two residues (Gln 767 and Met 769) of the hinge region of the EGFR kinase (dual hydrogen bond donor–acceptor system).<sup>22</sup>

—A chlorophenyl moiety occupying the region of the protein which is binding the ribose ring of ATP (“sugar pocket”). In addition, a sulfur–aromatic interaction between this moiety and residue Cys 773 of the pocket is assumed.<sup>18</sup>

—And optionally, groups filling a hydrophobic pocket extending in the direction of the lone pair of the N7 nitrogen of the adenine moiety of ATP. This pocket is present but not occupied in most protein kinases.

This pharmacophore model was fully consistent with a model of the EGFR PTK constructed by homology to the X-ray crystal structure of the cyclic-AMP-dependent protein kinase.<sup>25</sup>

Several flavonoid compounds have been reported to possess protein kinase inhibitory activity. The most prominent are genistein (**1**), quercetin (**2**), and flavopiridol (**3a**) (Chart 1). Due to its substantial potency (micromolar) in inhibiting the EGFR PTK, we considered **1** as a possible lead structure, and we were therefore interested in modeling its kinase binding mode. The three compounds **1–3** share a 5-hydroxy-chromenone substructure suggesting similar binding modes. X-ray crystal structures of quercetin (**2**) in complex with the Hck tyrosine kinase<sup>26</sup> and of the deschloro analogue **3b** of flavopiridol in complex with CDK2<sup>27</sup> have recently been determined. These structures show that the inhibitors make the same hydrogen bonds with the hinge region of the kinase as the N1 and N6 nitrogens of ATP which is in agreement with our pharmacophore model. In the flavopiridol analogue **3b**, these hydrogen bonds involved the keto function as an acceptor and the 5-hydroxy group of the chromenone system as a donor. In quercetin (**2**), the keto function also serves as a hydrogen bond acceptor; however, in this case the donor is the 3-hydroxy group. As a consequence, the region of the binding site occupied by the 2-phenyl substituent of the chromenone moiety is not the same for these two inhibitors (Figure 1). Their binding modes differ despite the fact that they belong to the same chemical class. On the basis of this information, we attempted to dock genistein (**1**) in the ATP-binding site of our EGFR kinase model, giving its 5-hydroxychromenone moiety the same two orientations as those seen in the above complexes. In both cases, we observed severe steric clashes between the *p*-hydroxyphenyl moiety in the 3-position and protein residues of the hinge region, suggesting the existence of a third binding mode specific to genistein.

A clue to the possible nature of this third binding mode came by comparing genistein (**1**) to the (phenyl-amino)quinazoline inhibitor class (compound **4**) reported by Zeneca and Parke-Davis.<sup>12,13</sup> In the literature, we found an example of enzyme inhibitors where a

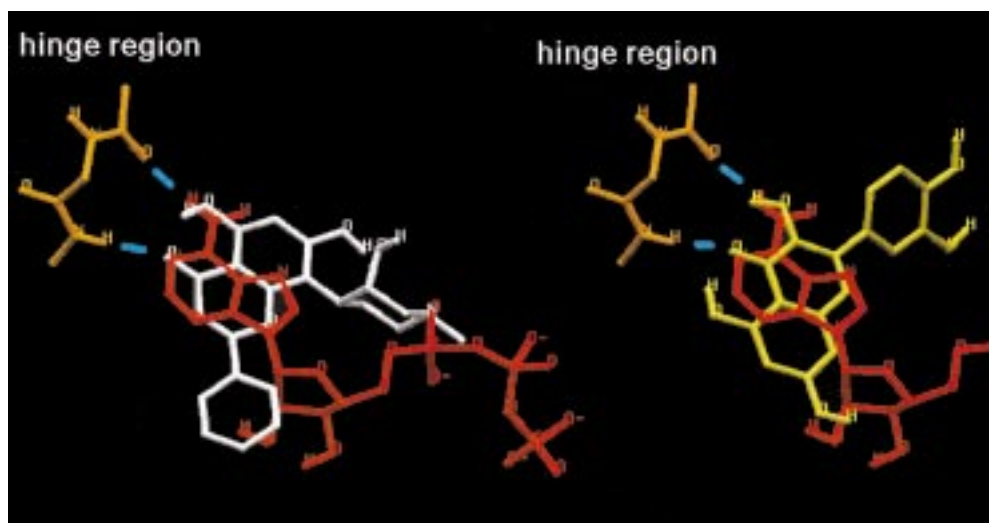


**Figure 1.** Binding modes of deschloroflavopiridol (**3b**) (white) and quercetin (**2**) (yellow) as compared to ATP (red). Hydrogen bonds appear as blue lines.

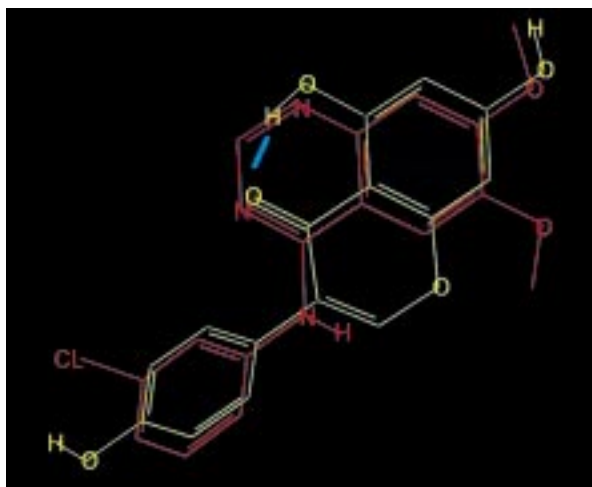


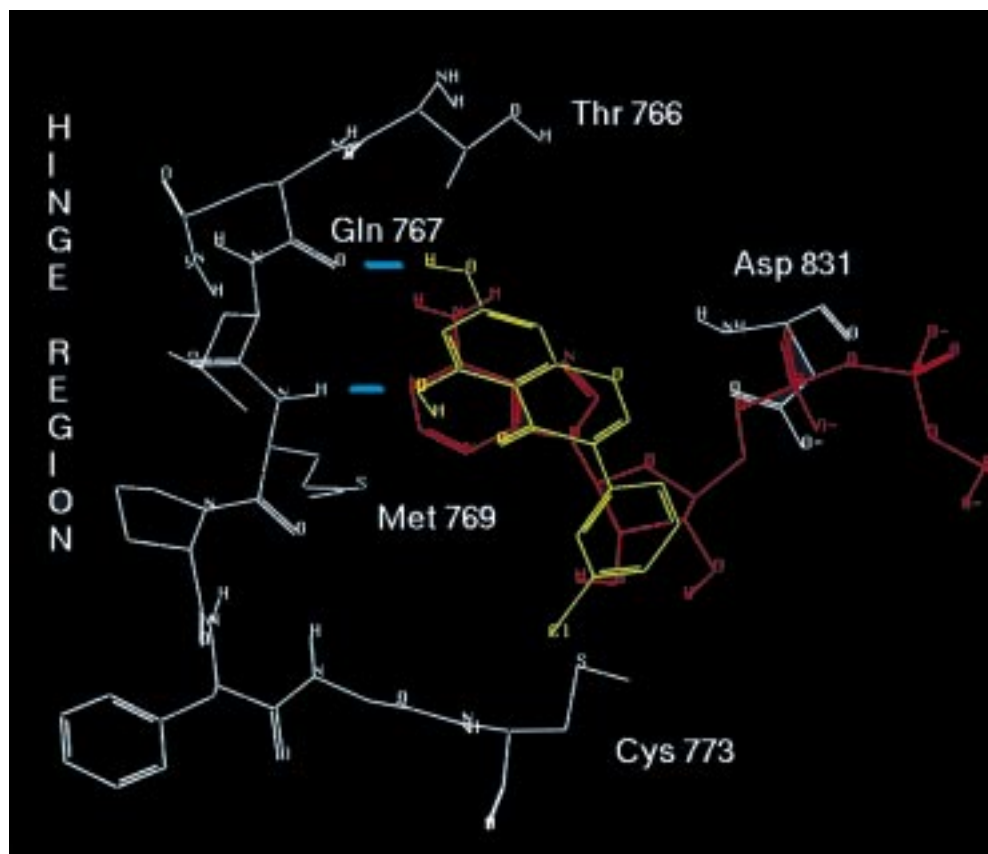
**Figure 2.** Superimposition of quinazoline **4** (red) with genistein (**1**) (yellow). The intramolecular hydrogen bond present in genistein appears in blue.

salicylic group has been reported to be a successful bioisosteric replacement of a quinazoline moiety.<sup>28</sup> Thereby, the pyrimidine ring mimics the pseudo-six-membered ring resulting from the hydroxy-keto intramolecular hydrogen bond in salicylic acid. A similar hydroxy-keto function is present in genistein (**1**). Assuming the same bioisosteric relationship between the quinazoline-type EGFR kinase inhibitors and genistein (**1**) led to the hypothesis that they share a common binding mode. In Figure 2 it can be seen that overlapping the 5-hydroxy-keto system of genistein (**1**) and the

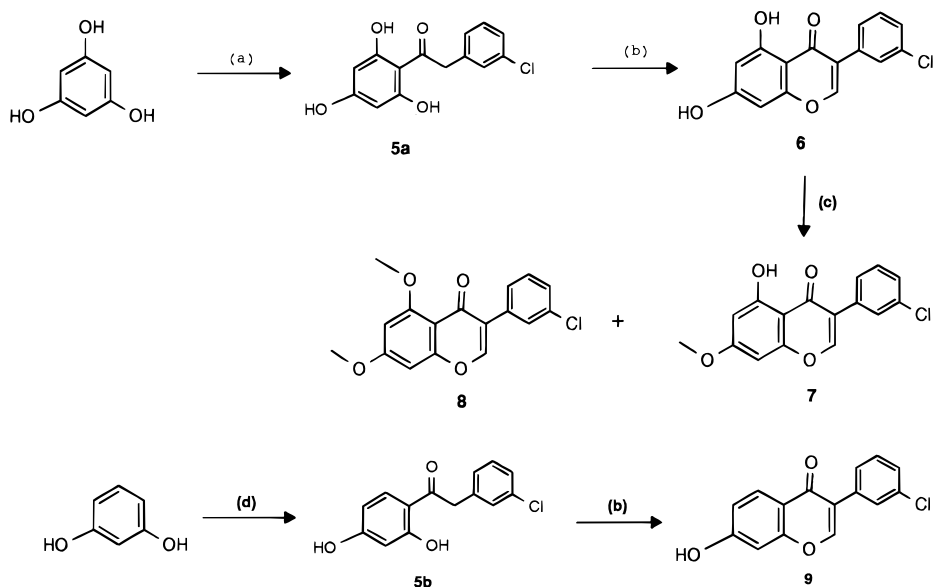
pyrimidine ring of **4** gives a very good overall superimposition of the two molecules. In particular, the anilino moiety of **4** superimposes nicely on the *p*-hydroxyphenyl group of genistein. Given the importance of the anilino *m*-chloro substituent in conferring high EGFR PTK inhibitory activity to the quinazoline derivatives,<sup>13</sup> as well as to the other classes of (phenylamino)pyrimidine inhibitors (e.g., (phenylamino)pyrrolopyrimidines<sup>18</sup> and (phenylamino)pyrazolopyrimidines<sup>19</sup>), the overlay shown in Figure 2 immediately suggested that replacing the *p*-hydroxyphenyl moiety of genistein by a *m*-chlorophenyl ring would enhance its potency. This idea motivated the synthesis of compound **6** as a first target structure.

A representation of the putative binding mode of **6** in the ATP-binding site of our EGFR kinase model is shown in Figure 3. Consistent with our pharmacophore model, we assumed that the chlorophenyl ring fits in the "sugar pocket" making a sulfur–aromatic interaction with Cys 773. Mimicking ATP, the 5-hydroxy substituent accepts a hydrogen bond from the backbone NH of residue Met 769, while the 7-hydroxy substituent donates a hydrogen bond to the backbone carbonyl of Gln 767. It can be seen that in this binding mode, the orientation of the chromenone moiety of **6** is such that oxygen O1 approximately occupies the region of the binding site corresponding to the C8 atom of the adenine ring of ATP. This oxygen atom is thus facing the part of the cavity binding the triphosphate chain of ATP.

On the basis of this putative binding mode, we suggested that replacement of O1 by a nitrogen atom would allow the attachment of groups that may give rise to beneficial interactions with amino acids of the tri-



**Figure 3.** Putative binding mode of compound **6**: compound **6** (yellow) superimposed on ATP (red). Hydrogen bonds appear as blue lines.

**Scheme 1.** Synthesis of Isoflavones<sup>a</sup>

<sup>a</sup> Reagents and conditions: (a) 3-chlorobenzyl cyanide, ZnCl<sub>2</sub>, HCl, ether, room temperature, 4 h; (b) CH<sub>3</sub>SO<sub>2</sub>Cl, DMF, BF<sub>3</sub>·O(C<sub>2</sub>H<sub>5</sub>)<sub>2</sub>, 100 °C, 2 h; (c) diazomethane, methanol; (d) 3-chlorophenylacetyl chloride, SnCl<sub>4</sub>, room temperature, 18 h.

phosphate binding part of the cavity. The quinolone derivatives **11**–**15** were synthesized following this concept.

**Chemistry**

**Synthesis of Isoflavones.** 3'-Chloro-5,7-dihydroxyisoflavone (**6**) was synthesized according to a published procedure (Scheme 1).<sup>29</sup> Reaction of phloroglucinol with 3-chlorobenzyl cyanide by the Houben–Hoesch method gave trihydroxyphenyl benzyl ketone **5a**.<sup>30</sup> **5a** was converted to the isoflavone **6** by Vilsmeier–Haack type reaction in 95% yield. The monomethyl ether **7** and dimethyl ether **8** were obtained by reaction of **6** with diazomethane in methanol. In analogy to **6**, 3'-chloro-7-hydroxyisoflavone (**9**) was obtained from **5b** via Vilsmeier–Haack reaction.

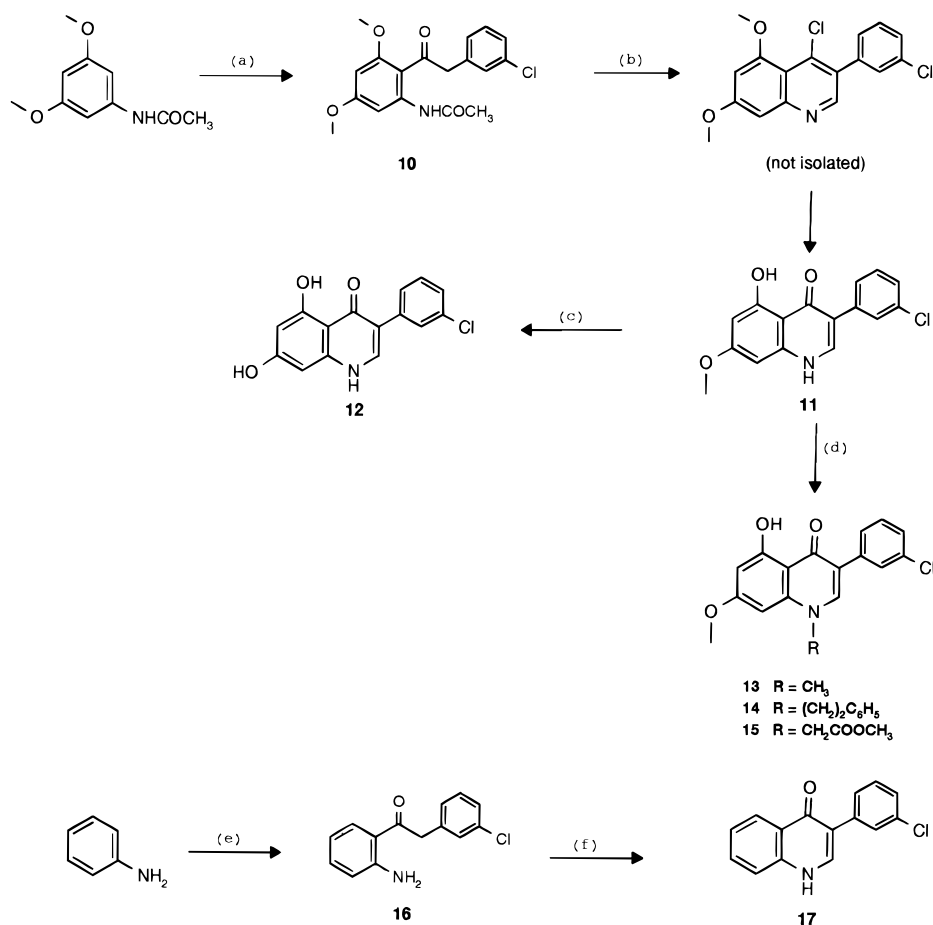
**Synthesis of 3-Aryl-4(1*H*)-quinolones.** The synthesis of 3-aryl-4(1*H*)-quinolones was based on the Vilsmeier–Haack reaction as used for the synthesis of the isoflavones. The target compound 3-(3-chlorophenyl)-5-hydroxy-7-methoxy-4(1*H*)-quinolone (**11**) was synthesized in two steps starting from *N*-(3,5-dimethoxyphenyl)acetamide (obtained from 3,5-dimethoxyaniline by acetylation) (Scheme 2). Friedel–Crafts alkylation of the acetamide with (3-chlorophenyl)acetyl chloride gave the ketone intermediate **10** in 65% yield (together with its regioisomer). Ring closure of the ketone **10** under modified Vilsmeier–Haack conditions (POCl<sub>3</sub>, DMF) directly gave the desired quinolone **11** in 42% yield. 5,7-Dihydroxy-4(1*H*)-quinolone **12** was obtained from **11** by ether cleavage with boron tribromide in toluene.

The *N*-alkylated quinolones **13**–**15** were obtained by reaction of **11** with the corresponding alkyl halide and potassium carbonate in DMF. Alkylation of **12** under the same conditions failed. In a similar way as described for compound **11**, 3-(3-chlorophenyl)-4(1*H*)-quinolone (**17**) was synthesized in two steps by Friedel–Crafts alkylation of aniline with 3-chlorobenzyl cyanide to the ketone **16**, followed by ring closure to the final quinolone **17**.

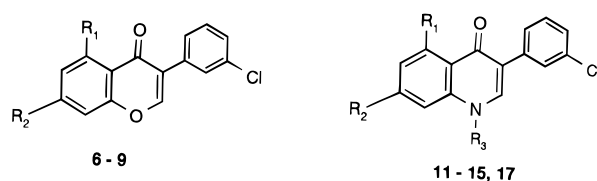
**Biological Evaluation and Discussion**

Genistein (**1**), the isoflavones **6**–**9**, and the quinolones **11**–**15** and **17** were tested against the intracellular domain of the EGFR tyrosine according to assay conditions described in detail in the literature (Table 1).<sup>31</sup> As predicted, the target compound **6** (IC<sub>50</sub> = 95 nM) was approximately 10 times more potent than **1**. The 7-methoxy derivative **7** (IC<sub>50</sub> = 1.27 μM) was less active than **6** indicating that modifications at this position decrease potency. In the model, the 7-hydroxy substituent of **6** donates a hydrogen bond to the backbone carbonyl of residue Gln 767, which is no longer possible with a methoxy group. Abolishing this interaction seems to be detrimental for kinase inhibition. The 5,7-dimethoxy derivative **8** and compound **9**, where the 5-hydroxy group is missing, were inactive (IC<sub>50</sub> > 100 μM), thus proving that the 5-hydroxy function is essential for biological activity. We assumed that this substituent accepts an important hydrogen bond from residue Met 769 of the kinase. The loss of activity observed upon its deletion in compound **9** was thus expected. With regard to the replacement of the 5-hydroxy group by a methoxy group, it was expected to have a more dramatic effect on the activity than in the case of the 7-hydroxyl substituent. In the 7-position, the CH<sub>3</sub> of the methoxy group can be oriented in the opposite direction to the 7-hydroxy proton of **6** forming the hydrogen bond, thus avoiding a steric clash with the backbone carbonyl of Gln 767. In addition, it is conceivable that the methoxy oxygen atom can still accept a hydrogen bond from the side chain of the adjacent Thr 766 residue. In contrast, due to the presence of the proximal keto function that imposes a steric restriction, a methoxy substituent in the 5-position must have its methyl group oriented toward the backbone NH of residue Met 769, therefore causing a steric clash with the protein.

Replacement of the oxygen in the chromane ring system of compound **6** by a nitrogen (compound **12**) further improved the inhibitory activity against the EGFR kinase by a factor of more than 10. With an IC<sub>50</sub>

**Scheme 2.** Synthesis of Quinolones<sup>a</sup>

<sup>a</sup> Reagents and conditions: (a) 3-chlorophenylacetyl chloride, SnCl<sub>4</sub>, room temperature, 3 h; (b) POCl<sub>3</sub>, DMF, 72 h, 80 °C; (c) PBr<sub>3</sub>, toluene, reflux, 18 h; (d) alkyl halide, K<sub>2</sub>CO<sub>3</sub>, DMF, room temperature; (e) 3-chlorobenzyl cyanide, BCl<sub>3</sub>, AlCl<sub>3</sub>; CH<sub>3</sub>SO<sub>2</sub>Cl, DMF, BF<sub>3</sub>·O(C<sub>2</sub>H<sub>5</sub>)<sub>2</sub>, 80 °C, 3 h.

**Table 1.** EGFR Tyrosine Kinase Activity and in Vitro Selectivity of Derivatives

compd	R <sub>1</sub>	R <sub>2</sub>	R <sub>3</sub>	formula	EGFR <sup>a</sup>	v-Abl <sup>a</sup>	c-Src <sup>a</sup>	PKC-α <sup>a</sup>
<b>1</b>					1.0	> 10	> 10	> 100
<b>4</b>					0.006	0.125	2.70	> 100
<b>6</b>	OH	OH		C <sub>15</sub> H <sub>9</sub> ClO <sub>4</sub>	0.095	20	> 100	> 100
<b>7</b>	OH	OCH <sub>3</sub>		C <sub>16</sub> H <sub>11</sub> ClO <sub>4</sub>	1.27	> 100	> 100	> 100
<b>8</b>	OCH <sub>3</sub>	OCH <sub>3</sub>		C <sub>17</sub> H <sub>13</sub> ClO <sub>4</sub>	500	nt	nt	nt
<b>9</b>	H	OH		C <sub>15</sub> H <sub>9</sub> ClO <sub>3</sub>	58.8	nt	nt	nt
<b>11</b>	OH	OCH <sub>3</sub>		C <sub>16</sub> H <sub>12</sub> ClNO <sub>3</sub>	0.038	> 100	> 100	> 100
<b>12</b>	OH	OH		C <sub>15</sub> H <sub>10</sub> ClNO <sub>3</sub>	0.008	> 10	8.0	> 100
<b>13</b>	OH	OCH <sub>3</sub>	CH <sub>3</sub>	C <sub>17</sub> H <sub>14</sub> ClNO <sub>3</sub>	0.170	> 10	> 10	> 100
<b>14</b>	OH	OCH <sub>3</sub>	(CH <sub>2</sub> ) <sub>2</sub> C <sub>6</sub> H <sub>5</sub>	C <sub>24</sub> H <sub>20</sub> ClNO <sub>3</sub>	4.0	nt	nt	nt
<b>15</b>	OH	OCH <sub>3</sub>	CH <sub>2</sub> COOCH <sub>3</sub>	C <sub>19</sub> H <sub>16</sub> ClNO <sub>5</sub>	0.064	> 10	> 10	> 100
<b>17</b>	H	H		C <sub>15</sub> H <sub>10</sub> ClNO	> 100	nt	nt	nt

<sup>a</sup> Expressed in IC<sub>50</sub> values (μM). Average of at least three determinations with <30% variability.

value of 8 nM, this compound was the most potent one of this series and was under our assay conditions as potent as the quinazoline **4**. As already observed in the isoflavone series, the 7-methoxyquinolone **11** (IC<sub>50</sub> = 38 nM) was less active than compound **12**. Docking of compound **12** into the EGFR PTK model according to our binding mode hypothesis suggests the possibility of

a direct or water-mediated hydrogen bond between the quinolone NH group of **12** and amino acid Asp 831 of the protein depending on the rotameric state chosen for the side chain of the latter. Again, and in accordance with our model, removal of the 5-hydroxy function together with the 7-hydroxy group (compound **17**) led to a complete loss of activity (IC<sub>50</sub> > 100 μM).

**Table 2.** Cellular Activity of Compounds

compd	inhibition of EGF-dependent phosphorylation <sup>a</sup>	inhibition of PDGF-dependent phosphorylation <sup>a</sup>	inhibition of MK cell proliferation <sup>a</sup>
<b>1</b>			
<b>4</b>	0.12	> 10	<0.1
<b>6</b>	12.0	> 10	16.0
<b>7</b>	> 100	> 10	45.2
<b>8</b>	> 100	> 10	46.2
<b>11</b>	6.0	> 10	11.4
<b>12</b>	2.0	> 10	10.2
<b>13</b>	3.0	> 10	2.83
<b>14</b>	1.5	> 10	4.93
<b>15</b>	12.5	> 10	9.55

<sup>a</sup> Expressed in IC<sub>50</sub> values ( $\mu$ M). Average of at least three determinations with <30% variability.

According to the proposed binding mode, the nitrogen of **12** points into the direction of the triphosphate region of ATP. Therefore, this nitrogen should be susceptible for modifications if one assumes a certain flexibility of Asp 831, the amino acid of the protein most proximal to this position. Although the activity against the EGFR kinase could not be improved by *N*-alkylation (compounds **13–15**), the best compound **15** of this series had an IC<sub>50</sub> value of 64 nM and was more potent than the simple methyl compound **13** (IC<sub>50</sub> = 170 nM), indicating that there is a chance to further improve the potency with a more polar substituent at the nitrogen, capable of forming an additional interaction with an amino acid in the triphosphate region.

All tested compounds showed high selectivity against other tyrosine kinases (v-Abl, c-Src) and against the serine/threonine kinase PKC- $\alpha$ .

When the inhibition of phosphorylation was tested on a cellular level, only the quinolone **14** (IC<sub>50</sub> = 1.5  $\mu$ M) and to a certain extent compounds **11** (IC<sub>50</sub> = 6  $\mu$ M), **12** (IC<sub>50</sub> = 2  $\mu$ M), and **13** (IC<sub>50</sub> = 3  $\mu$ M) showed satisfactory but not exciting inhibitory activities. However, all four compounds did not inhibit PDGF-dependent phosphorylation (IC<sub>50</sub> values > 10  $\mu$ M), thereby indicating selectivity for the EGF-mediated signal transduction pathway. None of the compounds were very potent in the inhibition of the proliferation of the EGF-dependent mouse keratinocyte MK cell line. The best compounds **13** and **14** had IC<sub>50</sub> values of 2.83 and 4.9  $\mu$ M, respectively (Table 2). On the basis of these results, none of the compounds were further tested in vivo.

The activity profiles of the isoflavones **6** and **7** and especially of the quinolones **11** and **12** show that our pharmacophore model of the ATP-binding site together with additional rational approaches can successfully be used for the design of novel classes of highly potent and selective EGFR tyrosine kinase inhibitors.

It is implicit in what is described above that we assumed that the quinazoline inhibitor **4** conforms to our pharmacophore model (its N1 atom accepts a hydrogen bond from Met 769, while its anilino moiety occupies the sugar pocket). Parke-Davis scientists have proposed a different binding mode for the quinazoline inhibitors.<sup>23</sup> In their model the N1 atom still makes the hydrogen bond with Met 769; however, the anilino moiety fits in the large hydrophobic pocket extending in the direction of the lone pair of the N7 atom of the adenine moiety of ATP. We think that both models can account for most of the existing structure–activity

relationships. In both cases, the gain in binding affinity produced by a chloro or bromo substituent in the meta position of the anilino moiety is explained by a sulfur–aromatic interaction with a cysteine residue of the protein (Cys 773 in our model and Cys 751 in the Parke-Davis model). It is our conviction that depending on the substitution pattern and the nature of the substituents, the quinazoline and related inhibitors can adopt either one of the two binding modes. X-ray crystal structures of CDK2 complexed with different ligands have clearly shown that molecules belonging to the same chemical class (adenine derivatives) can bind to the kinase in different orientations depending on the substitution pattern.<sup>32</sup> For the isoflavone and quinolone inhibitors described in this work, a better interpretation of the structure–activity data is obtained assuming that they adopt the binding mode of our model, but the compounds can also be docked in the EGFR kinase model according to Parke-Davis' binding mode without producing steric clashes and structural inconsistencies.

## Experimental Section

**Kinase Assays.** Purification of protein kinases and in vitro enzyme tests were performed as previously described<sup>33,34</sup> using poly(E<sub>4</sub>Y) (2  $\mu$ g/mL) and [<sup>33</sup>P]ATP (0.4  $\mu$ M) as substrates. All compounds were dissolved in DMSO and diluted in buffer, giving a final DMSO concentration of 1% in the assay. IC<sub>50</sub> values represent averages of at least three determinations. Genistein (IC<sub>50</sub> = 1  $\mu$ M) and the dianilinophthalimide CGP 52411 (IC<sub>50</sub> = 1  $\mu$ M) served as an internal standard inhibitor in all EGFR kinase assays.

**Inhibition of Cellular Tyrosine Phosphorylation.** Inhibition of EGF- and PDGF-stimulated total cellular tyrosine phosphorylation in A431 cells and BALB/c 3T3 cells, respectively, was measured using a microtiter ELISA assay as previously reported.<sup>28,29</sup> Under our assay conditions, EGF or PDGF stimulation caused a 3–4-fold increase in tyrosine or substrate phosphorylation.

**Antiproliferative Assays.** Assays were performed essentially as previously described.<sup>35</sup> Drug (in a final DMSO concentration of 0.5%) was added 24 h after plating, and growth was monitored after 3–5 days of incubation using methylene blue staining. Cell growth of nonadherent cells was monitored by using the calorimetric MTT assay. IC<sub>50</sub> was defined as the drug concentration causing a 50% reduction of signal as compared to control cultures which contain identical solvent concentrations (100%). IC<sub>50</sub> values represent the mean of at least two independent assays using serial dilutions of the drug diluted with culture medium.

**Synthesis.** Elemental analyses were within  $\pm$ 0.4% of the theoretical value. <sup>1</sup>H NMR spectra were recorded on a Varian Gemini 300 spectrometer. The chemical shifts are reported in parts per million (ppm) downfield from tetramethylsilane (TMS). Splitting patterns are designated as follows: s, singlet; brs, broad singlet; d, doublet; t, triplet; q, quartet; m, multiplet. <sup>13</sup>C NMR spectra were recorded on a Varian Gemini 300 spectrometer. Chemical shifts are reported in ppm downfield from TMS. Multiplicities observable with off-resonance decoupling were obtained from <sup>1</sup>H, <sup>13</sup>C shift correlated spectra (HETCOR) and are denoted with s, d, t, q (see above); the number of hydrogen atoms bound directly to carbon as obtained from attached proton test experiments is denoted with e, even; o, odd. Mass spectra (MS) were recorded on a VG 70-250 mass spectrometer. Analytical thin-layer chromatography (TLC) was carried out on precoated plates (silica gel, 60 F-254, Merck), and spots were visualized with UV light or iodine. Flash chromatography was carried out with Merck silica gel 60 (40–63  $\mu$ m) and Chemische Fabrik Uetikon silica gel (30–70  $\mu$ m). HPLC was carried out using a Waters system (Waters controller 600 and Waters photodiode array detector)

with Millenium 2010 software. Melting points were measured on a Kofler block and are uncorrected.

**2-(3-Chlorophenyl)-1-(2,4,6-trihydroxyphenyl)ethanone (5a).** An amount of 9.2 g (72.9 mmol) of phloroglucinol (1,3,5-trihydroxybenzene) and 11.05 g (72.9 mmol) of 3-chlorobenzyl cyanide were dissolved in 70 mL of anhydrous ether. Zinc chloride was added, and a stream of dry hydrogen chloride was bubbled through the reaction mixture for 4 h. A viscous yellowish mass has separated from the slightly brown solution. The flask was left closed overnight, and then the ethereal layer was removed by decantation; 150 mL of 2 M HCl was added, and the partly dissolved mass was heated to 100 °C for 2.5 h. The hot solution was filtered and the yellow solid collected. A lower second phase formed in the filtrate as a brown oil, which crystallized upon cooling to give 14.05 g of the crude product (69% yield). Crystallization from ethyl acetate/pentane gave **5a** as light-yellow crystals: mp 182.6–184.7 °C; <sup>1</sup>H NMR (DMSO-*d*<sub>6</sub>) δ 12.25 (brs, 2H), 10.52 (brs, 1H), 8.49 (s, 1H), 7.35–7.19 (m, 4H), 5.900 (s, 1H), 4.898 (s, 1H), 4.40 (s, 2H); <sup>13</sup>C NMR (DMSO-*d*<sub>6</sub>) 201.5 (e), 165.0 (e), 164.3 (e, 2 C), 138.4 (e), 132.7 (e), 129.74 (o), 129.66 (o), 128.4 (o), 126.2 (o), 103.7 (e), 94.8 (o, 2 C), 48.6 (e); CIMS (NH<sub>3</sub>) *m/z* 279 (M + H)<sup>+</sup>. Anal. (C<sub>14</sub>H<sub>11</sub>ClO<sub>4</sub>) N; C: calcd, 60.34; found, 61.50. H: calcd, 3.98; found, 3.27.

**2-(3-Chlorophenyl)-1-(4,6-dihydroxyphenyl)ethanone (5b).** To a solution of 1.3 mL (11.20 mmol) of stannic chloride in 12 mL of 1,2-dichloroethane was added dropwise at room temperature a solution of 695 mg (3.68 mmol) of 3-chlorophenylacetyl chloride in 12 mL of 1,2-dichloroethane; 385 mg (3.5 mmol) of resorcinol was added in small portions. The solution was heated until all added resorcinol had dissolved and was stirred at room temperature overnight. The solution was poured onto ice and the organic phase diluted with methylene chloride. The organic phase was washed with water, dried, and evaporated. The reddish oily residue was purified by flash chromatography (toluene/ethyl acetate, 9:1) giving 366 mg (40% yield) of **5b** which was used without further purification: <sup>1</sup>H NMR (DMSO-*d*<sub>6</sub>) δ 12.61 (s, 1H), 10.91 (brs, 1H), 8.13 (d, 1H), 7.57–7.43 (m, 4H), 6.63 (dd, 1H), 6.51 (d, 1H), 4.54 (s, 2H); <sup>13</sup>C NMR (DMSO-*d*<sub>6</sub>) 201.2, 165.1, 164.5, 137.6, 133.4, 132.9, 130.0, 129.6, 128.5, 126.6, 112.3, 108.4, 102.6, 43.6.

**3'-Chloro-5,7-dihydroxyisoflavone (6).** An amount of 5.06 g (18.16 mmol) of the ketone **5a** was dissolved in 40 mL of DMF; 14 mL (109 mmol) of boron trifluoride etherate was carefully added; 4.5 mL (54.5 mmol) of methanesulfonyl chloride, dissolved in 40 mL of DMF, was added to the ketone-etherate mixture. The red solution was heated at 100 °C for 2 h and then poured onto ice, thereby forming a yellowish mixture which gave an off-white precipitate after a few hours. The precipitate was collected by filtration, dissolved in ethyl acetate, and washed with water. The organic phase was dried over sodium sulfate and evaporated to dryness yielding a red oil which was purified by flash chromatography using toluene/ethyl acetate (6:4) as eluent; 5.15 g (95% yield) of the isoflavone **6** were obtained which after crystallization from ethanol/water gave fine off-white needles: mp 182.4–184.5 °C; <sup>1</sup>H NMR (DMSO-*d*<sub>6</sub>) δ 12.76 (s, 1H), 10.95 (brs, 1H), 8.49 (s, 1H), 7.67 (s, 1H), 7.57–7.46 (m, 3H), 6.42 (d, 1H), 6.25 (d, 1H); <sup>13</sup>C NMR (DMSO-*d*<sub>6</sub>) 179.4 (e), 164.5 (e), 161.9 (e), 157.5 (e), 155.5 (o), 132.9 (e), 132.8 (e), 129.9 (o), 128.5 (o), 127.8 (o), 127.5 (o), 120.8 (e), 104.3 (e), 99.2 (o), 93.8 (o); EIMS *m/z* 288 (M<sup>+</sup>). Anal. (C<sub>15</sub>H<sub>9</sub>ClO<sub>4</sub>) C, H, N, O.

**3'-Chloro-5-hydroxy-7-methoxyisoflavone (7) and 3'-Chloro-5,7-dimethoxyisoflavone (8).** An amount of 0.12 g (0.426 mmol) of **6** was dissolved in 6 mL of methanol and cooled to –20 °C; 10 mL of an ethereal solution of diazomethane was added, and the reaction mixture stirred for 4 days at –14 °C. The solution was evaporated to dryness and the residue dissolved in ethyl acetate/water. The organic phase was washed with water, dried, and evaporated. The crude yellow solid was purified by flash chromatography (toluene/ethyl acetate, 6:4) to give 0.11 g (85% yield) of **7**. Crystallization from toluene gave yellowish crystals: mp 147.5–150.2 °C; <sup>1</sup>H NMR

(DMSO-*d*<sub>6</sub>) δ 12.76 (s, 1H), 8.59 (s, 1H), 7.68 (t, 1H), 7.56–7.46 (m, 3H), 6.70 (d, 1H), 6.44 (d, 1H), 3.88 (s, 3H); <sup>13</sup>C NMR (DMSO-*d*<sub>6</sub>) 179.6 (e), 165.4 (e), 161.6 (e), 157.4 (e), 155.9 (o), 132.8 (e), 129.9 (o), 128.5 (o), 126.9 (o), 127.5 (o), 121.0 (e), 105.3 (e), 98.2 (o), 92.6 (o), 56.1 (o); EIMS *m/z* 302 (M<sup>+</sup>). Anal. (C<sub>16</sub>H<sub>11</sub>ClO<sub>4</sub>) C, H, N, O.

A total of 8.4 mg (6% yield) of **8** of mp 107–112 °C was isolated as a byproduct: EIMS *m/z* 316 (M<sup>+</sup>), corresponding to C<sub>17</sub>H<sub>13</sub>ClO<sub>4</sub>; <sup>1</sup>H NMR (DMSO-*d*<sub>6</sub>) δ 8.31 (s, 1H), 7.60 (s, 1H), 7.48–7.32 (m, 3H), 6.64 (d, 1H), 6.50 (d, 1H), 3.87 (s, 3H), 3.84 (s, 3H); <sup>13</sup>C NMR (DMSO-*d*<sub>6</sub>) 173.1 (e), 163.7 (e), 160.8 (e), 159.1 (e), 152.2 (o), 134.3 (e), 132.6 (e), 129.7 (o), 128.7 (o), 127.5 (o), 127.4 (o), 123.5 (e), 108.8 (e), 96.2 (o), 92.9 (o), 56.0 (o), 55.9 (o). Anal. (C<sub>17</sub>H<sub>13</sub>ClO<sub>4</sub>) H, N, O; C: calcd, 64.46; found, 63.64.

**3'-Chloro-7-hydroxyisoflavone (9).** An amount of 0.42 mL (3.30 mmol) of boron trifluoride etherate was added dropwise to a solution of 144 mg (0.55 mmol) of the ketone **5b** in 1.3 mL of DMF. Then, 0.13 mL (1.65 mmol) of methanesulfonyl chloride in 1.3 mL of DMF was added dropwise. The reaction mixture was heated at 100 °C for 2 h and then hydrolyzed by pouring onto ice. After standing overnight, a yellow precipitate had formed which was filtered off (Celite). The residue was dissolved in ethyl acetate; the organic solution was washed with water, dried, and evaporated. The yellowish oily residue was purified by flash chromatography (toluene/ethyl acetate, 9:1) to give 85 mg (57% yield) of **9** as yellowish crystals: mp 243.5–246.5 °C; <sup>1</sup>H NMR (DMSO-*d*<sub>6</sub>) δ 10.90 (brs, 1H), 8.49 (s, 1H), 7.99 (d, 1H), 7.68 (s, 1H), 7.57–7.38 (m, 3H), 6.97 (dd, 1H), 6.90 (d, 1H); <sup>13</sup>C NMR (DMSO-*d*<sub>6</sub>) 174.0, 162.7, 157.3, 154.4, 134.2, 132.6, 129.9, 128.5, 127.5, 127.4, 127.2, 122.0, 116.4, 115.3, 102.1; EIMS *m/z* 272 (M<sup>+</sup>), corresponding to C<sub>15</sub>H<sub>9</sub>ClO<sub>3</sub>.

**2-(3-Chlorophenyl)-1-(6-acetamido-2,4-dimethoxyphenyl)ethanone (10).** An amount of 0.27 g (1.39 mmol) of *N*-(3,5-dimethoxyphenyl)acetamide (obtained from 3,5-dimethoxyaniline by acetylation with acetic anhydride) was partially dissolved in 50 mL of 1,2-dichloroethane and cooled to 0 °C; 0.33 mL (2.77 mmol) of stannic chloride was added. Finally, 0.315 g (1.66 mmol) of (3-chlorophenyl)acetyl chloride was added over 15 min at room temperature. The yellow-brown reaction mixture was stirred at room temperature for 3 h, then poured onto ice, and extracted with methylene chloride. The organic phase was washed with water, dried, and evaporated to dryness to yield a brown oil which was purified by flash chromatography (toluene/ethyl acetate, 6:4) to yield 0.31 g (65% yield) of crude yellowish product. Crystallization from toluene gave off-white needles of **10**: mp 110–112.5 °C; <sup>1</sup>H NMR (CDCl<sub>3</sub>) δ 11.42 (brs, 1H), 7.97 (d, 1H), 7.27–7.20 (m, 3H), 7.07 (dd, 1H), 6.18 (d, 1H), 4.22 (s, 2H), 3.85 (s, 6H), 1.26 (s, 3H); <sup>13</sup>C NMR (CDCl<sub>3</sub>) 201.5 (e), 169.6 (e), 164.8 (e), 161.9 (e), 143.5 (e), 137.9 (e), 134.0 (e), 129.8 (o), 129.5 (o), 127.8 (o), 126.8 (o), 108.2 (e), 97.1 (o), 94.1 (o), 55.6 (o), 55.5 (o), 50.9 (e), 25.7 (o); EIMS *m/z* 347 (M<sup>+</sup>). Anal. (C<sub>18</sub>H<sub>18</sub>ClNO<sub>4</sub>) C, H, N, O.

The isomeric 2-(3-chlorophenyl)-1-(4-acetamido-2,6-dimethoxyphenyl)ethanone was isolated as a byproduct (yellow needles from toluene of mp 154.3–157.1 °C).

**3-(3-Chlorophenyl)-5-hydroxy-7-methoxy-4(1H)-quinolone (11).** DMF (1 mL) was cooled to 10 °C, 0.74 mL (9.67 mmol) of phosphorus oxychloride was added, and the reaction mixture was stirred at room temperature for 30 min, thereby developing a deep-pink color; 2.80 g (8.06 mmol) of **10** in 2 mL of DMF was added to the DMF–POCl<sub>3</sub> complex, upon which the reaction mixture turned deep red. The mixture was stirred for 1 h at room temperature and then for 72 h at 80 °C, cooled to room temperature, and finally poured onto ice. The dark-brown residue was purified by flash chromatography (toluene/ethyl acetate, 6:4) yielding 1.02 g of crude product (42% yield). Crystallization from DMF gave fine yellow needles **11**: mp 268.5–271.6 °C; <sup>1</sup>H NMR (DMSO-*d*<sub>6</sub>) δ 14.75 (s, 1H), 12.40 (brs, 1H), 8.25 (s, 1H), 7.81 (t, 1H), 7.66 (dd, 1H), 7.47–7.34 (m, 2H), 6.46 (d, 1H), 6.23 (d, 1H), 3.82 (s, 3H); <sup>13</sup>C NMR (DMSO-*d*<sub>6</sub>) 178.8 (s), 163.6 (s), 162.9 (s), 141.4 (s), 139.7 (d), 136.8 (s), 132.6 (s), 129.7 (d), 127.9 (d), 126.9 (d), 126.4 (d),

116.4 (s), 108.3 (s), 96.7 (d), 89.9 (d), 55.4 (q); EIMS  $m/z$  301 ( $M^+$ ). Anal. ( $C_{16}H_{12}ClNO_3$ ) C, H, N, O.

**3-(3-Chlorophenyl)-5,7-dihydroxy-4(1H)-quinolone (12).** An amount of 0.02 mL (1.03 mmol) of boron tribromide was added to a suspension of 81.5 mg (0.27 mmol) of the quinolone **11** in 10 mL of toluene and refluxed for 18 h. The dark-brown suspension was cooled to 0 °C and methanol added. The solution was evaporated and the residue triturated with diethyl ether, which was removed by decantation leaving a crude brown residue. Purification by flash chromatography (toluene/ethyl acetate, 6:4) gave 11.7 mg (15.5% yield) of **12** as a yellow solid: mp 145–147 °C;  $^1H$  NMR (DMSO- $d_6$ )  $\delta$  14.70 (s, 1H), 12.26 (d, 1H), 10.32 (s, 1H), 8.16 (d, 1H), 7.79 (t, 1H), 7.66–7.60 (m, 1H), 7.46–7.25 (m, 2H), 6.35 (d, 1H), 6.06 (d, 1H);  $^{13}C$  NMR (DMSO- $d_6$ ) 178.7, 163.0, 162.4, 141.6, 139.3, 137.0, 132.6, 129.7, 128.0, 126.8, 126.3, 115.9, 107.4, 97.8, 91.7; EIMS  $m/z$  287 ( $M^+$ ), corresponding to  $C_{15}H_{10}ClNO_3$ .

**3-(3-Chlorophenyl)-5-hydroxy-7-methoxy-N-methyl-4(1H)-quinolone (13).** An amount of 0.123 g (0.41 mmol) of 3-(3-chlorophenyl)-5-hydroxy-7-methoxy-4(1H)-quinolone (**11**) was dissolved in 4 mL of DMF. Then 0.03 mL (0.48 mmol) of methyl iodide and 0.1 g (1 mmol) of potassium carbonate were added. The reaction mixture was stirred at room temperature for 30 min, poured into water, and extracted with ethyl acetate. The organic phase was dried and the solvent removed in vacuo to yield 0.12 g (93% yield) of a yellow solid. Crystallization from toluene gave **13** as fine yellow needles: mp 177.4–183.0 °C;  $^1H$  NMR (DMSO- $d_6$ )  $\delta$  15.27 (s, 1H), 8.40 (s, 1H), 7.80 (t, 1H), 7.70–7.66 (m, 1H), 7.46–7.37 (m, 2H), 6.45 (d, 1H), 6.33 (d, 1H), 3.88 (s, 3H), 3.85 (s, 3H);  $^{13}C$  NMR (DMSO- $d_6$ ) 178.1 (e), 163.9 (e), 163.9 (e), 145.1 (o), 141.9 (e), 136.5 (e), 132.7 (e), 129.7 (o), 127.9 (o), 126.8 (o), 126.5 (o), 116.1 (e), 108.3 (e), 96.9 (o), 89.7 (o), 55.6 (o), 41.0 (o); EIMS  $m/z$  315 ( $M^+$ ). Anal. ( $C_{17}H_{14}ClNO_3$ ) C, H, N, O.

**3-(3-Chlorophenyl)-5-hydroxy-7-methoxy-N-(2-phenylethyl)-4(1H)-quinolone (14).** Quinolone **11** (60 mg, 0.198 mmol) was dissolved in 5 mL of DMF. Then, 0.1 mL (0.74 mmol) of 2-phenylethyl bromide and 0.1 g (1 mmol) of potassium carbonate were added. The reaction mixture was stirred at room temperature for 17 h, then poured into water and extracted with ethyl acetate. The organic phase was dried and the solvent removed in vacuo to yield 74 mg of a yellow oil. Purification by flash chromatography (toluene/ethyl acetate, 9:1) and crystallization from toluene gave 43 mg (63% yield) of **14** (mp 142.6–144.5 °C) in the form of yellow needles:  $^1H$  NMR ( $CDCl_3$ )  $\delta$  15.11 (s, 1H), 7.34–7.02 (m, 10H), 6.38 (d, 1H), 6.31 (d, 1H), 4.27 (t, 2H), 3.88 (s, 3H), 3.14 (t, 2H);  $^{13}C$  NMR ( $CDCl_3$ ) 179.2 (e), 165.7 (e), 164.6 (e), 142.8 (o), 140.9 (e), 136.9 (e), 135.9 (e), 134.0 (e), 129.3 (o), 129.2 (o, 2 C), 129.0 (o, 2 C), 128.4 (o), 127.6 (o), 127.1, 126.8 (o), 125.3 (o), 118.1 (e), 109.2 (e), 96.4 (o), 89.7 (o), 55.6 (o), 55.5 (e), 34.3 (e); EIMS  $m/z$  405 ( $M^+$ ). Anal. ( $C_{24}H_{20}ClNO_3$ ) C, H, N, O.

**Methyl [3-(3-Chlorophenyl)-5-hydroxy-7-methoxy-4-oxo-4H-quinolin-1-yl]acetate (15).** Prepared in analogy to **13** and **14**. From 0.1 g (0.332 mmol) of the quinolone **11** and 0.032 mL (0.332 mmol) of bromoacetic acid methyl ester, 69 mg (52% yield) of **15** was obtained as yellow needles: mp 151.4–156.5 °C (crystallization from toluene);  $^1H$  NMR ( $CDCl_3$ )  $\delta$  14.82 (s, 1H), 7.57–7.40 (m, 3H), 7.22–7.32 (m, 2H), 6.33 (d, 1H), 5.97 (d, 1H), 4.72 (s, 2H), 3.82 (s, 3H), 3.80 (s, 3H);  $^{13}C$  NMR ( $CDCl_3$ ) 179.6 (e), 167.3 (e), 165.2 (e), 164.7 (e), 142.8 (o), 141.6 (e), 135.6 (e), 134.1 (e), 129.5 (o), 128.5 (o), 127.5 (o), 126.8 (o), 119.4 (e), 108.8 (e), 96.7 (o), 89.4 (o), 55.6 (o), 54.4 (e), 53.2 (o); EIMS  $m/z$  373 ( $M^+$ ). Anal. ( $C_{19}H_{16}ClNO_5$ ) C, H, N, O.

**1-(2-Aminophenyl)-2-(3-chlorophenyl)ethanone (16).** Freshly distilled aniline (2.2 mL, 23 mmol) dissolved in 25 mL of 1,2-dichloroethane was added dropwise to a solution of 25.3 mL (25.3 mmol) of  $BCl_3$  in dichloromethane cooled to 0 °C; 5.9 mL (46 mmol) of 3-chlorobenzyl cyanide and 3.37 g (25.3 mmol) of  $AlCl_3$  were added to the white suspension, and the reaction mixture was stirred at 80 °C for 20 h and cooled to 0 °C; 2 N HCl was added to the brown mixture, upon which a yellow precipitate formed. The mixture was then refluxed for 30 min

at 80 °C and extracted with dichloromethane. The organic phase was washed with 1 M NaOH, dried, and evaporated to yield 8.4 g of a yellow oil, which consisted of a mixture of product **16** and residual 3-chlorobenzyl cyanide, which could not be separated. The crude product was used for the next step without further purification:  $^1H$  NMR ( $CDCl_3$ )  $\delta$  7.79 (dd, 1H), 7.38–7.10 (m, 5H), 6.69–6.62 (m, 2H), 6.3 (brs, 1H); GCMS  $m/z$  245 ( $M^+$ ).

**3-(3-Chlorophenyl)-4(1H)-quinolone (17).** To the mixture of the ketone **16** and 3-chlorobenzyl cyanide (2.77 g, 4.76 mmol) was carefully added boron trifluoride etherate (4.16 mL, 33.1 mmol). Methanesulfonyl chloride (1.28 mL, 16.6 mmol) was added, and the reaction mixture was heated to 80 °C for 3 h and then poured onto 1 M NaOH. The precipitate so formed was collected by filtration, washed with water and toluene, dispersed in hot hexane, filtered, and dried in vacuo to yield 717.4 mg of crude product. This was adsorbed on silica gel, which then was washed with toluene/ethyl acetate (3:2) for removal of the starting materials. Desorption of **17** was achieved by refluxing the silica gel with ethyl acetate. The adsorbent was removed by filtration and the filtrate dried and evaporated. The residue obtained was washed with acetone to give 310 mg (21% yield) of quinolone **17** as a white powder: mp 300–301 °C;  $^1H$  NMR (DMSO- $d_6$ )  $\delta$  12.1 (brs, 1H), 8.28 (s, 1H), 8.23 (d, 1H), 7.92 (t, 1H), 7.74–7.59 (m, 3H), 7.47–7.30 (m, 3H);  $^{13}C$  NMR (DMSO- $d_6$ ) 174.5 (e), 139.2 (e), 138.7 (o), 138.3 (e), 132.5 (e), 131.8 (o), 129.6 (o), 127.9 (o), 126.6 (o), 126.1 (o), 125.9 (e), 125.6 (o), 123.5 (o), 118.3 (o), 117.9 (e); EIMS  $m/z$  255 ( $M^+$ ). Anal. ( $C_{15}H_{10}ClNO$ ) C, H, N, O.

**Acknowledgment.** We gratefully acknowledge the contributions of Andreas Wicki and Roland K. Sigel for the synthesis of compounds **5a**, **9**, **16**, and **17** and the excellent technical assistance of B. Adam, U. Duerler, I. Oberkirch, R. Reuter, and R. Roth.

## References

- (1) Aaronson, S. A. Growth Factors and Cancer. *Science* **1991**, *254*, 1146–1152.
- (2) Fry, D. W.; Kraker, A. J.; Connors, R. C.; Elliott, W. L.; Nelson, J. M.; Showalter, H. D.; Leopold, W. R. Strategies for the discovery of novel tyrosine kinase inhibitors with anticancer activity. *Anti-Cancer Drug Des.* **1994**, *9*, 331–351.
- (3) Levitzki, A.; Gazit, A. Tyrosine Kinase Inhibition: An Approach to Drug Development. *Science* **1995**, *267*, 1782–88.
- (4) Ullrich, A.; Schlessinger, J. Signal Transduction by Receptors with Tyrosine Kinase Activity. *Cell* **1990**, *61*, 203–212.
- (5) Elder, J. T.; Fisher, G. J.; Lindquist, P. B.; Bennett, G. L.; Pittelkow, M. R.; Coffey, R. J.; Ellingsworth, L.; Derynck, R.; Voorhees, J. J. Overexpression of transforming growth factor  $\alpha$  in psoriatic epidermis. *Science* **1989**, *243*, 811–814.
- (6) Fry, D. W. Protein tyrosine kinases as therapeutic targets in cancer chemotherapy and recent advances in the development of new inhibitors. *Exp. Opin. Invest. Drugs* **1994**, *3*, 577–595.
- (7) Traxler, P.; Lydon, N. Recent Advances in Protein Tyrosine Kinase Inhibitors. *Drugs Future* **1995**, *20*, 1261–1274.
- (8) Spada, A. P.; Myers, M. R. Small molecule inhibitors of tyrosine kinase activity. *Exp. Opin. Ther. Patents* **1995**, *5*, 805–817.
- (9) Bridges, A. J. The current status of tyrosine kinase inhibitors: do the diarylamine inhibitors of the EGF receptor represent a new beginning? *Exp. Opin. Ther. Patents* **1995**, *5*, 1245–1257.
- (10) Traxler, P. Protein tyrosine kinase inhibitors in cancer treatment. *Exp. Opin. Ther. Patents* **1997**, *7*, 571–588.
- (11) Ward, W. H. J.; Cook, P. N.; Slater, A. M.; Davies, D. H.; Holdgate, G. A.; Green, L. R. Epidermal growth factor receptor tyrosine kinase. Investigation of catalytic mechanism, structure-based searching and discovery of a potent inhibitor. *Biochem. Pharmacol.* **1994**, *48*, 659–666.
- (12) Fry, D. W.; Kraker, A. J.; McMichael, A.; Ambrosio, L. A.; Nelson, J. M.; Leopold, W. R.; Connors, R. W.; Bridges, A. J. A Specific Inhibitor of the Epidermal Growth Factor Receptor Tyrosine Kinase. *Science* **1994**, *265*, 1093–1095.
- (13) Rewcastle, G. W.; Denny, W. A.; Bridges, A. J.; Zhou, H.; Cody, D. R.; McMichael, A.; Fry, D. W. Tyrosine Kinase Inhibitors. 5. Synthesis and Structure–Activity Relationships for 4-(Phenylmethyl-amino)- and 4-(Phenylamino)quinazolines as Potent Adenosine 5'-Triphosphate Binding Site Inhibitors of the Tyrosine Kinase Domain of the Epidermal Growth Factor Receptor. *J. Med. Chem.* **1995**, *38*, 3482–3487.



- (14) Rewcastle, G. W.; Palmer, B. D.; Bridges, A. J.; Showalter, H. D.; Sun, L.; Nelson, J. M.; McMichael, A.; Kraker, A. J.; Fry, D. W.; Denny, W. A. Tyrosine kinase inhibitors. 9. Synthesis and evaluation of fused tricyclic quinazolines analogues as ATP site inhibitors of the tyrosine kinase activity of the epidermal growth factor receptor. *J. Med. Chem.* **1996**, *39*, 918–928.
- (15) Thompson, A. M.; Bridges, A. J.; Fry, D. W.; Kraker, A. J.; Denny, W. A. Tyrosine Kinase Inhibitors. 7. 7-Amino-4-(phenylamino)- and 7-Amino-4-[(phenyl-methyl)amino]-pyrido[4,3-d]pyrimidines: A New Class of Inhibitors of the Tyrosine Kinase Activity of the Epidermal Growth Factor Receptor. *J. Med. Chem.* **1995**, *38*, 3780–3788.
- (16) Rewcastle, G. W.; Palmer, B. D.; Thompson, A. M.; Bridges, A. J.; Cody, D. R.; Zhou, H.; Fry, D. W.; McMichael, A.; Kraker, A. J.; Denny, W. A. Tyrosine Kinase Inhibitors. 10. Isomeric 4-[(3-bromophenyl)-amino]pyrido[d]-pyrimidines are potent ATP binding site inhibitors of the tyrosine kinase function of the epidermal growth factor receptor. *J. Med. Chem.* **1996**, *39*, 1823–1835.
- (17) Rewcastle, G. W.; Bridges, A. J.; Fry, D. W.; Rubin, J. A.; Denny, W. A. Tyrosine kinase inhibitors. 12. Synthesis and structure-activity relationships for 6-substituted- 4-(phenylamino)pyrimido[5,4-d]pyrimidines designed as inhibitors of the epidermal growth factor receptor. *J. Med. Chem.* **1997**, *40*, 1820–1826.
- (18) Traxler, P.; Furet, P.; Mett, H.; Buchdunger, E.; Meyer, T.; Lydon, N. 4-(Phenylamino)pyrrolopyrimidines: Potent and Selective, ATP Site Directed Inhibitors of the EGF-Receptor Protein Tyrosine Kinase. *J. Med. Chem.* **1996**, *38*, 2285–2292.
- (19) Traxler, P.; Bold, G.; Frei, J.; Lang, M.; Lydon, N.; Mett, H.; Buchdunger, E.; Meyer, T.; Mueller, M.; Furet, P. Use of a Pharmacophore Model for the Design of EGF-R Tyrosine Kinase Inhibitors: 4-(Phenylamino)Pyrazolo-Pyrimidines. *J. Med. Chem.* **1997**, *40*, 3601–3616.
- (20) Woodburn, J. R.; Barker, A. J.; Gibson, K. H.; Ashton, S. E.; Wakeling, A. E.; Curry, B. J.; Scarlett, L.; Henthorn, L. R. ZD1839, an epidermal growth factor tyrosine kinase inhibitor selected for clinical development. *Proc. Am. Cancer Res.* **1997**, *38*, 6633.
- (21) Moyer, J. D.; Barbacci, E. G.; Iwata, K. K.; Arnold, L.; Boman, B.; Cunningham, A.; Diorio, C.; Doty, J.; Morin, M. J.; Moyer, M. P.; Neveu, M.; Pollack, V. A.; Pustilnik, L. R.; Reynolds, M. M.; Sloan, D.; Theleman, A.; Miller, P. Induction of Apoptosis and Cell Cycle Arrest by CP-358 774, an Inhibitor of Epidermal Growth Factor Receptor Tyrosine Kinase. *Cancer Res.* **1997**, *57*, 4838–4848.
- (22) Furet, P.; Caravatti, G.; Lydon, N.; Priestle, J.; Sowadski, J.; Trinks, U.; Traxler, P. Modeling Study of Protein Kinase Inhibitors: Binding Mode of Staurosporine – Origin of the Selectivity of CGP 52 411. *J. Comput.-Aided Mol. Des.* **1995**, *9*, 465–471.
- (23) Palmer, B. D.; Trumpp-Kallmeyer, S.; Fry, D. W.; Nelson, J. M.; Showalter, H. D. H.; Denny, W. A. Tyrosine Kinase Inhibitors. 11. Soluble Analogues of Pyrrolo- and Pyrazoloquinazolines as Epidermal Growth Factor Receptor Inhibitors: Synthesis, Biological Evaluation, and Modeling of the Mode of Binding. *J. Med. Chem.* **1997**, *40*, 1519–1529.
- (24) Trumpp-Kallmeyer, S.; Rubin, J. R.; Humblet, C.; Hamby, J. M.; Showalter, H. D. H. Development of a Binding Model to Protein Tyrosine Kinases for Substituted Pyrido[2,3-d]pyrimidine Inhibitors. *J. Med. Chem.* **1998**, *41*, 1752–1763.
- (25) Zheng, J.; Knighton, D. R.; Ten Eyck, L. F.; Karlsson, R.; Xuong, N. H.; Taylor, S. S.; Sowadski, J. M. Crystal Structure of the Catalytic Subunit of cAMP-Dependent Protein Kinase Complexed with MgATP and Peptide Inhibitor. *Biochemistry* **1993**, *32*, 2154–2161.
- (26) Siccheri, F.; Moarefi, I.; Kuriyan, J. Crystal structure of the Src family tyrosine kinase Hck. *Nature* **1997**, *385*, 602–609.
- (27) Filgueira de Azevedo, W., Jr.; Mueller-Dieckmann, H. J.; Schulze-Gahmen, U.; Worland, P. J.; Sausville, E.; Kim, S.-H. Structural basis for specificity and potency of a flavanoid inhibitor of human CDK2, a cell cycle kinase. *Proc. Natl. Acad. Sci. U.S.A.* **1996**, *93*, 2735–2740.
- (28) Hodge, C. N.; Pierce, J. A. diazine heterocycle replaces a six-membered hydrogen-bonded array in the active site of scytalone dehydratase. *Bioorg. Med. Chem. Lett.* **1993**, *3*, 1605–1608.
- (29) Bass, R. J. Verfahren zur Herstellung von 4-Oxo-4H-benzopyranderivaten, 4-Oxo-4H-benzopyranderivate und ihre Verwendung in Futtermitteln. Deutsches Patentamt, Offenlegungsschrift 26 40 617, 1977.
- (30) Chapman, E.; Stephen, H. Di- and Tri-hydroxydeoxybenzoins. *J. Chem. Soc.* **1923**, 404–409.
- (31) Buchdunger, E.; Trinks, U.; Mett, H.; Regenass, U.; Müller, M.; Meyer, Th.; McGlynn, E.; Pinna, L. A.; Traxler, P.; Lydon, N. B. 4,5-Dianilino-phthalimide: A protein-tyrosine kinase inhibitor with selectivity for the epidermal growth factor receptor signal transduction pathway and potent in vivo antitumor activity. *Proc. Natl. Acad. Sci. U.S.A.* **1994**, *91*, 2334–2338.
- (32) Schulze-Gahmen, U.; Brandsen, J.; Jones, H. D.; Morgan, D. O.; Meijer, L.; Vesely, J.; Kim, S. H. Multiple Modes of Ligand Recognition: Crystal Structures of Cyclin-Dependent Protein Kinase 2 in Complex with ATP and Two Inhibitors, Olomoucine and Isopentenyladenine. *Proteins* **1995**, *22*, 378–391.
- (33) Buchdunger, E.; Trinks, U.; Mett, H.; Regenass, U.; Müller, M.; Meyer, Th.; Beilstein, P.; Wirz, B.; Schneider, P.; Traxler, P.; Lydon, N. B. 4,5-Bis(4-fluoro-anilino)-phthalimide: a selective inhibitor of the EGF receptor signal transduction pathway with potent in vivo antitumor activity. *Clin. Cancer Res.* **1995**, *1*, 813–821.
- (34) Buchdunger, E.; Zimmermann, J.; Mett, H.; Meyer, Th.; Müller, M.; Regenass, U.; Lydon, N. B. Selective inhibition of the platelet-derived growth factor signal transduction pathway by a protein-tyrosine kinase inhibitor of the 2-phenylaminopyrimidine class. *Proc. Natl. Acad. Sci. U.S.A.* **1995**, *92*, 2558–2562.
- (35) Meyer, T.; Regenass, U.; Fabbro, D.; Alteri, E.; Roesel, J.; Mueller, M.; Caravatti, G.; Matter, A. A derivative of staurosporine (CGP 41 251) shows selectivity for protein kinase C inhibition and in vitro proliferative as well as in vivo antitumor activity. *Int. J. Cancer* **1989**, *43*, 851–856.

JM9805510